Tight focusing of femtosecond elliptically polarised vortex light pulses*

Hua Li-Min(华黎闽), Chen Bao-Suan(陈宝算), Chen Zi-Yang(陈子阳), and Pu Ji-Xiong(蒲继雄)†

College of Information Science and Engineering, Institute of Optics and Photonics, Huaqiao University, Quanzhou 362021, *China*

(Received 28 May 2010; revised manuscript received 1 July 2010)

This paper studies the tight focusing properties of femtosecond elliptically polarised vortex light pulses. Based on Richards–Wolf vectorial diffraction integral, the expressions for the electric field, the velocity of the femtosecond light pulse and the total angular momentum of focused pluses are derived. The numerical calculations are also given to illustrate the intensity distribution, phase contour, the group velocity variation and the total angular momentum near the focus. It finds that near the focus the femtosecond elliptically polarised vortex light pulse can travel at various group speeds, that is, slower or faster than light speed in vacuum, depending on the numerical aperture of the focusing objective system. Moreover, it also studies the influence of the numerical aperture of the focusing objective and the time duration of the elliptically polarised vortex light pulse on the total angular momentum distribution in the focused field.

Keywords: tight focusing, ultrashort pulse, elliptically polarised, vectorial Debye integral

PACS: 42.25.Fx, 42.25.Ja, 42.30.Kq **DOI:** 10.1088/1674-1056/20/1/014202

1. Introduction

When light is focused by a high numerical aperture (NA) objective, the light beam can be focused into an extremely small spot, and has a strong longitudinal component created near the focus.[1−5] Due to these special properties, tight focusing has wide potential applications, such as optical data storage, microscopy, material processing, and particle trapping.[6−9] On the other hand, optical vortices and vortex beams have attracted vast attention as a new branch of modern optics for several years.[10] This kind of beams has helical phase distribution and orbital angular momentum.[11,12] Therefore, the vortex beams have been investigated extensively for their wide applications, such as micromanipulation, optical spanner, and quantum information.[13−17]

Femtosecond light pulses, with special properties in increasing the temporal and spatial resolution which can be used in optical measurements, have been extensively studied.[18−25] Moreover, slow and fast light phenomena have attracted a growing interest over the last decade.[26−30] However, to the best of our knowledge, there are no papers studying the tight focusing of femtosecond elliptically polarised vortex light pulses. Therefore, it is of great interest to reveal the influence of variant elliptically polarised state on the focused vortex light pluses. In this paper, we want to study the tight focusing of the femtosecond vortex light pulses. The intensity distribution, the group velocity variation and the total angular momentum near the focus are investigated in detail by using numerical calculations.

2. Theory

Let us first consider the x-direction or y-direction linear-polarised Laguerre–Gaussian (LG) femtosecond light pulse as the vortex model. The electric field of such a pulse can be expressed as

$$\begin{aligned} & E_j(\rho,\varphi,t) \\ &= E_{0j}\left(\frac{\sqrt{2}\rho}{w_0}\right)^{|m|}\exp\left(-\frac{\rho^2}{w_0^2}\right)\exp(\mathrm{i}m\varphi)A(t), \\ & (j=x,y) \end{aligned} \tag{1}$$

where E_{0i} and w_0 are the constant amplitude and beam size respectively, $\exp(\mathrm{i}m\varphi)$ is the vortex phase factor and m is the topological charge, $A(t)$ is the temporal pulse shape which we assume to have Gaussian

*Project supported by the National Natural Science Foundation of China (Grant No. 60977068), the Natural Science Foundation of Fujian Province, China (Grant No. A0810012), and the Open Research Fund of State Key Laboratory of Transient Optics and Photonics, Chinese Academy of Sciences (Grant No. SKLST200912).

†Corresponding author. E-mail: jixiong@hqu.edu.cn

© 2011 Chinese Physical Society and IOP Publishing Ltd

profile, i.e.[31]

$$A(t) = \exp[-(a_{\rm g}t/T)^2]\exp(-{\rm i}\omega_0 t), \tag{2}$$

where $a_{\rm g} = (2\ln 2)^{1/2}$, T is the pulse duration, and w_0 is its central angular frequency.

Since objectives are often designed to obey the sine condition,[19] $\rho = f\sin\theta$, where f is the focal length of the high NA objective, and θ is the NA angle, shown in Fig. 1. Therefore, the pupil apodisation function of the linearly polarised LG femtosecond light pulse can be expressed as[23]

$$\begin{aligned} & S_j(\theta,\varphi,\omega) \\ &= \frac{1}{\sqrt{2\pi}}\int_{-\infty}^{\infty} E(\rho,\varphi,t)\exp({\rm i}\omega t)\,{\rm d}t \\ &= \frac{T}{\sqrt{2}a_{\rm g}}E_0\left(\frac{\sqrt{2}f\sin\theta}{w_0}\right)^{|m|}\exp\left(-\frac{(f\sin\theta)^2}{w_0^2}\right) \\ &\quad\times\ \exp({\rm i}m\varphi)\exp[-T^2(\omega-\omega_0)^2/4a_{\rm g}^2], \\ &\quad (j=x,y). \end{aligned} \tag{3}$$

Here we consider the incident pulse as an elliptically polarised LG femtosecond light pulse, the electric field can be expressed as

$$E_{\pm}(\rho) = E_x\boldsymbol{e}_x \pm E_y\,{\rm e}^{{\rm i}\beta}\boldsymbol{e}_y, \tag{4}$$

where $E_+(\rho)$ indicates the right-hand elliptical (RHE) polarised pulse, while $E_-(\rho)$ represents for the left-hand elliptical (LHE) polarisation, E_x and E_y are the electric fields of two orthogonal linear components, respectively, β is the retardation between the two components, $\boldsymbol{e}_x$ and $\boldsymbol{e}_y$ are unit vectors along the x and the y directions, respectively.

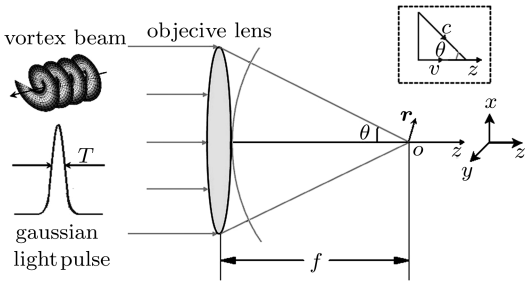


Fig. 1. Tight focusing system.

Then we use the above field distribution as illumination. The electric field of a single spectral component in the focal region when the light pulse is focused by a high NA objective is given by the Richards–Wolf vectorial diffraction method as[3,4,15,16]

$$\begin{aligned} E(r,\phi,z,\omega) &= \begin{bmatrix} E_x \pm E_x \\ E_y \pm E_y \\ E_z \pm E_z \end{bmatrix} \\ &= -\frac{{\rm i}kf}{2\pi}\int_0^{\theta_{\max}}\int_0^{2\pi}\exp[{\rm i}kr\sin\theta\cos(\varphi-\phi)+{\rm i}kz\cos\theta]\sin\theta\sqrt{\cos\theta} \\ &\quad\times\begin{bmatrix} S_x(\theta,\varphi,\omega)\left(\cos^2\varphi\cos\theta+\sin^2\varphi\right)\pm S_y(\theta,\varphi,\omega)\ {\rm e}^{{\rm i}\beta}\cos\varphi\sin\varphi(\cos\theta-1) \\ S_x(\theta,\varphi,\omega)\cos\varphi\sin\varphi(\cos\theta-1)\pm S_y(\theta,\varphi,\omega)\ {\rm e}^{{\rm i}\beta}\left(\cos^2\varphi+\sin^2\varphi\cos\theta\right) \\ S_x(\theta,\varphi,\omega)\sin\theta\cos\varphi\pm S_y(\theta,\varphi,\omega)\ {\rm e}^{{\rm i}\beta}\sin\theta\sin\varphi \end{bmatrix}{\rm d}\varphi{\rm d}\theta, \end{aligned} \tag{5}$$

where $k=\omega/c$ is the wave number relating to the angular frequency of the light pulse and $c = 3\times10^8$ m/s is the velocity of light in vacuum, $\theta_{\max}$ is the largest numerical angle of the objective.

By a Fourier-transformation, the electric fields of the femtosecond pulse in the vicinity of the focal spot can be calculated by the superposition of each spectral component as[23]

$$\begin{aligned} & E_j(r,\phi,z,t) \\ &= \int_0^{\infty} E_j(r,\phi,z,\omega)\exp(-{\rm i}\omega t)\ {\rm d}\omega,\ (j=x,y,z). \end{aligned} \tag{6}$$

Then we obtain the total intensity near the focus as follows:

$$\begin{aligned} I(r,\phi,z,t) &= \sum_{j=x,y,z} I_j(r,\phi,z,t) \\ &= \sum_{j=x,y,z} |E_j(r,\phi,z,t)|^2. \end{aligned} \tag{7}$$

The centroid of the light beam can be defined as the weighted average of position by the local intensity. Therefore, we use the beam centroid here to define the average propagation distance of the pulse on axis[32]

$$z(t) = \frac{\int_{-\infty}^{\infty} z\int_0^{2\pi}\int_0^{\infty} I(r,\phi,z,t)\,{\rm d}r\,{\rm d}\phi\,{\rm d}z}{\int_{-\infty}^{\infty}\int_0^{2\pi}\int_0^{\infty} I(r,\phi,z,t)\,{\rm d}r\,{\rm d}\phi\,{\rm d}z}. \tag{8}$$

Then the group speed of the light pulse along the

z-axis can be expressed as

$$v(t) = \mathrm{d}z(t)/\mathrm{d}t. \tag{9}$$

As is known to all, the total angular momentum (AM) of beams can be divided into spin AM (SAM) and orbital AM (OAM). Beams with an $\exp(\mathrm{i}m\varphi)$ azimuthal phase structure carry OAM of $m\hbar$ per photon, so does the light pulses with similar azimuthal phase structure. However, it is impossible to separate the total angular momentum of the photon into an 'orbital' and 'spin' part exactly. So we investigate the total AM of the vortex light pulses. Since the vortex light pulse is focused by a high NA objective, the AM should be analysed under the nonparaxial condition suggested by[10,33]

$$\frac{J_z}{W} = \frac{(m+\sigma)}{\omega} + \frac{\sigma}{\omega}\frac{\int_0^k \mathrm{d}\kappa[|E(\kappa)|^2\,\kappa/(k^2-\kappa^2)]}{\int_0^k \mathrm{d}\kappa[|E(\kappa)|^2\,(2k^2-\kappa^2)/\kappa(k^2-\kappa^2)]}, \tag{10}$$

where $\kappa = k\sin\theta$, W is the energy per unit length of light pulse, ω is the angular frequency of the incident pulse, σ is the helicity of the light beam, $\sigma = 0$ for linear polarised light, $\sigma = +1$ for left-handed, $\sigma = -1$ stands for right-handed circularly polarised light, and $-1 < \sigma < +1$ describes elliptically polarised light respectively. Therefore, the total AM of the vortex light pulse can be written as

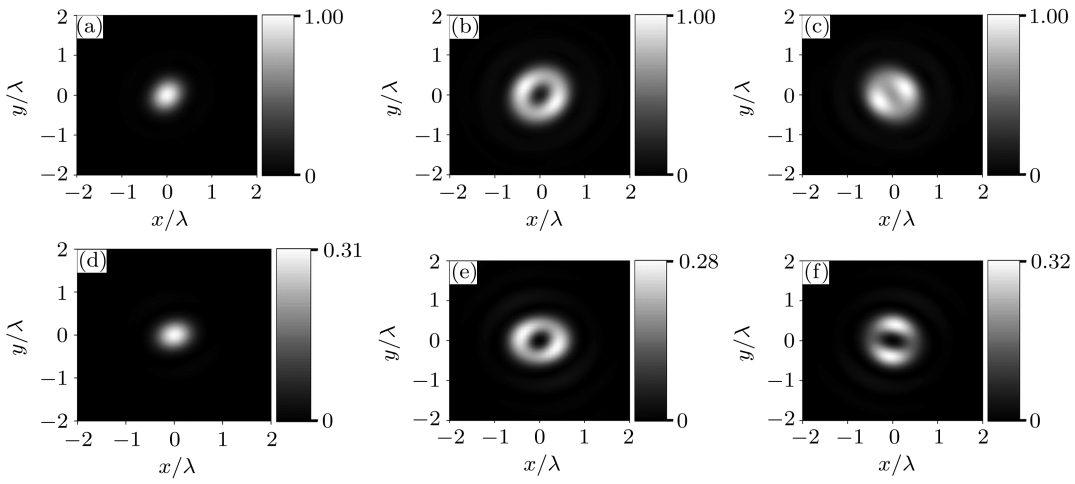
$$J_z = W \cdot \left[\frac{(m+\sigma)}{\omega} + \frac{\sigma}{\omega}\frac{\int_0^k \mathrm{d}\kappa[|E(\kappa)|^2\,\kappa/(k^2-\kappa^2)]}{\int_0^k \mathrm{d}\kappa[|E(\kappa)|^2\,(2k^2-\kappa^2)/\kappa(k^2-\kappa^2)]}\right]. \tag{11}$$

3. Results and discussions

Based on the above derived equations, we can perform some numerical calculations to illustrate the focusing properties of the femtosecond light pulse through a high NA objective. The parameters for the calculations are chosen to be $f = 1$ cm, and $w_0 = 2$ cm. We show in Fig. 2 the total intensity distribution and its x, y and z components in the focus for different topological charges and different polarisation directions. All the components are normalised to their total intensity, and all the position coordinates are normalised to the central wavelength ($\lambda = 249.1$ nm) of the femtosecond light pulse. It is shown that the focal spots are elliptical due to different amplitudes of the incident fields and the phase retardation between them.

It is shown in Figs. 2(a), 2(d), 2(g), and 2(j) that, for topological charge $m = 0$ (RHE-polarised pulse), the total intensity (I_t) and its x and y components (I_x and I_y) in the focus are nonzero at the centre, while the z component (I_z) has a zero central intensity.

For topological charge $m = 1$ (RHE-polarised pulse), as shown in Figs. 2(b), 2(e), 2(h), and 2(k), there is only one dark core for I_t, I_x and I_y. But the z component I_z has two at the same time, indicating that there are two vortices in the intensity distribution of the z component, which shows that the SAM can be converted into OAM.



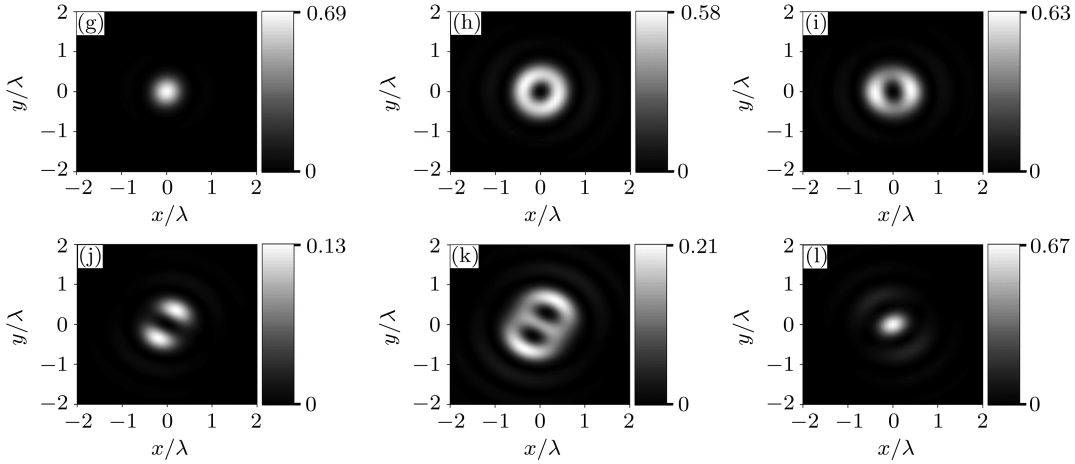


Fig. 2. The intensity distribution in the focus for focused beams with different topological charges. (a), (d), (g), (j) $m = 0$ (RHE-polarised pulse); (b), (e), (h), (k) $m = 1$ (RHE-polarised pulse); (c), (f), (i), (l) $m = 1$ (LHE-polarised pulse). (a)–(c) total intensity $I_{\rm t}$; (d)–(f) x component I_x; (g)–(i) y component I_y; (j)–(l) z component I_z. The other parameters are chosen as $T = 5$ fs, $\omega_0 = 7.57 \times 10^{15}$ s^{-1}, $\lambda = 249.1$ nm, NA $= 0.9$, $f = 1$ cm, $w_0 = 2$ cm, $\beta = \pi/4$, $E_{0x} = 1$, $E_{0y} = 1.5$.

The focusing properties for LHE-polarised pulse with $m = 1$ are shown in Figs. 2(c), 2(f), 2(i), and 2(l). Different from the RHE-polarised pulse, the central intensity of I_z is not hollow since the OAM is offset by the SAM of the LHE polarised pulse.

Figure 3 shows the phase contours of $E_z(r, \phi, z)$ with different topological charges in the focal plane. When topological charge $m = 0$, the phase contour of RHE-polarised pulse exhibits a counterclockwise distribution, which is shown in Fig. 3(a). Figure 3(b) shows that LHE-polarised pulse has a clockwise helical phase distribution. That is because the SAM of the incident pulse can be converted into the OAM in high NA focusing condition. The phase contour of $m = 1$ RHE-polarised pulse exhibit in Fig. 3(c) has two helical phases changing from $-\pi$ to π, therefore, its z-component intensity distribution has two dark cores, which is shown in Fig. 2(k). In Fig. 3(d), the centre of the phase contour is fixed, which means that the wavefront of the LHE-polarised pulse has no screw in the focal plane, and the centre of z-component intensity distribution is nonzero, as it is shown in Fig. 2(k). With the increase of the topological charge, the number of phase singularity in the focal plane is increased when the pulse is RHE-polarised, as it is shown in Figs. 3(a), 3(c), and 3(e). However, the

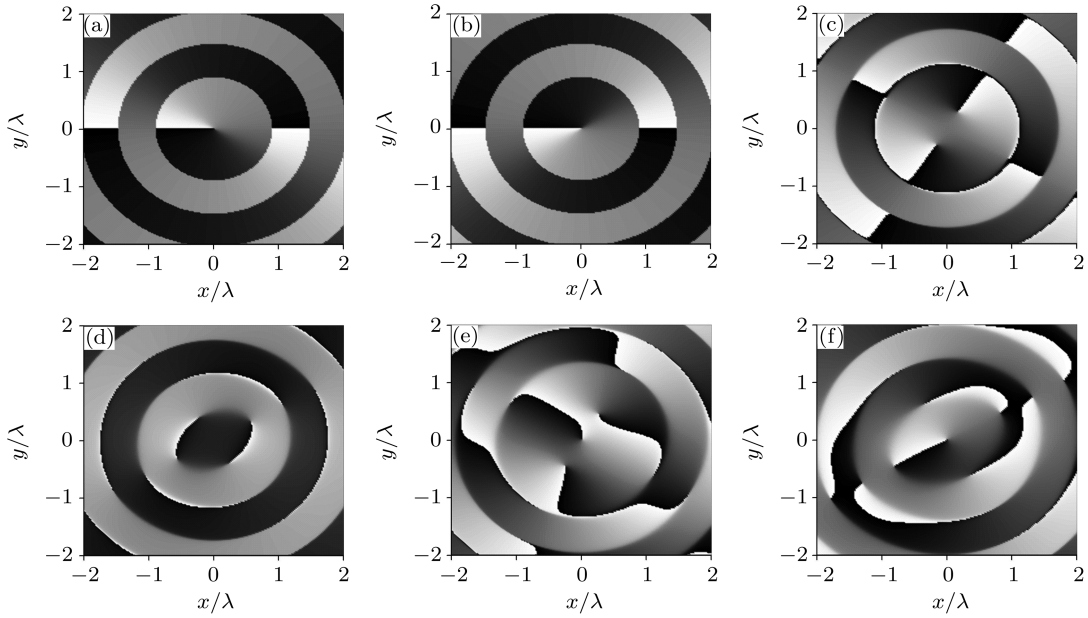


Fig. 3. Phase contours of $E_z(r, \phi, z)$ in the focal plane. (a), (b) $m = 0$; (c), (d) $m = 1$; (e), (f) $m = 2$; (a), (c), (e) RHE-polarised beam; (b), (d), (f) LHE-polarised beam. The other parameters are the same as those in Fig. 2.

number of phase singularity for the LHE-polarised decreases, which is shown in Figs. 3(b), 3(d), and 3(f). That is because for the RHE-polarised pulse, the OAM converted from SAM is in the same direction as the original OAM, thus the total OAM enhances, but for the LHE-polarised pulse, the OAM converted from SAM is in the opposite direction to the original OAM, so that the total OAM is reduced.

Phase contours of the x, y, and z components in the focal plane with $m = 1$ are indicated in Fig. 4. There is only one vortex in the phase contours of $E_x(r, \phi, z)$ and $E_y(r, \phi, z)$ of RHE- or LHE-polarised pulses. However, it is interesting to find that the phase contours of $E_z(r, \phi, z)$ exhibit a combined vortex for the RHE- polarised pulse, and no vortex for the LHE-polarised pulses, for the SAM to OAM conversion is more obvious in the phase distributions of $E_z(r, \phi, z)$.

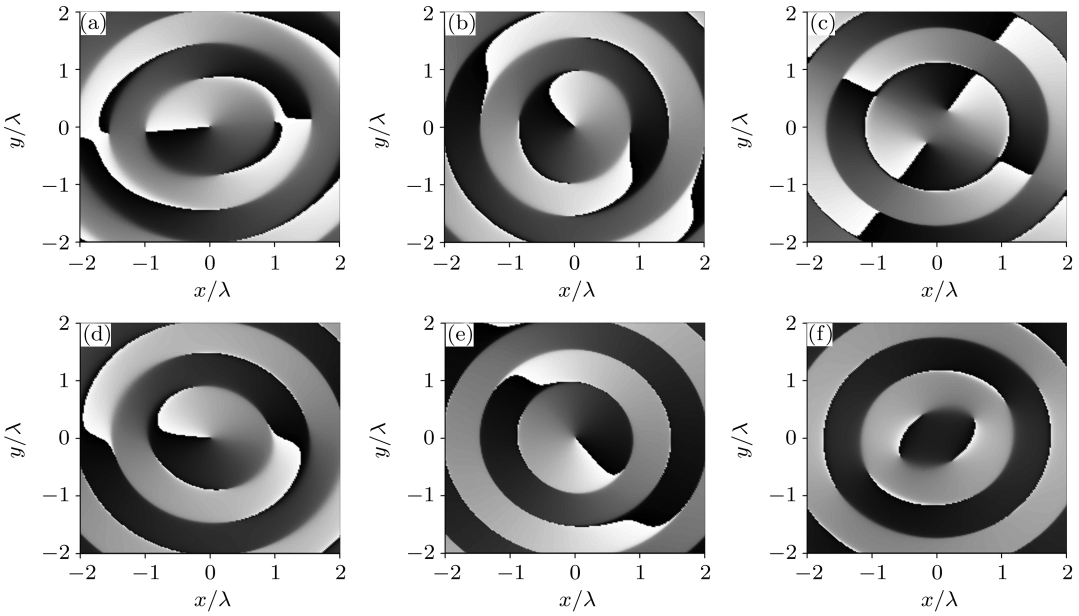


Fig. 4. Phase contours of the x, y, and z components in the focal plane with $m = 1$. (a), (b), (c) RHE-polarised pulse; (d), (e), (f) LHE-polarised pulse; (a), (d) $E_x(r, \phi, z)$; (b), (e) $E_y(r, \phi, z)$; (c), (f) $E_z(r, \phi, z)$. The other parameters are the same as those in Fig. 2.

The influence of varying phase retardation β on the phase distributions of $E_z(r, \phi, z)$ in the focal plane is shown in Fig. 5. It is found that with β changing from 0 to $\pi/2$, the two phase singularity will gradually become closer and closer, and get the least distance when $\beta = \pi/2$. Then by further increasing β, the two phase singularity will separate again. This means that the distance of the two vortex cores can be controlled by changing the value of phase retardation β.

Figure 6 illustrates the propagation evolution of the $m = 1$ RHE-polarised femtosecond vortex light pulse passing through a high NA objective. It is shown that there is a dark region along the z-axis, corresponding to the dark core in Fig. 2(b).

Moreover, we find that the light pulse propagates faster when it is far enough away from the focus and slows down near the focus. The more detailed group velocity variation is given in Fig. 7. The pulse group velocity is normalised to the velocity of light in vacuum $c = 3 \times 10^8$ m/s. It is shown that the total group velocity and the three component velocity all slow down to less than half of the velocity in vacuum at the focus. That is because in tight focusing process, the light pulse group velocity c is projected onto the z-axis as velocity $v(t)$, as shown in the inset in Fig. 1. This result is important since it offers a new technique to control the motion state of photons and enables research into controlling the interaction of light and materials.

Then we compare the total group velocity variation of light pulses with different topological charges in Fig. 8. It is found that the femtosecond vortex light pulse generally propagates slower than the non-vortex light pulse. And the larger the topological charge is, the smaller the group speed is, which indicates that the slow light phenomenon is more pronounced in femtosecond vortex light pulse.

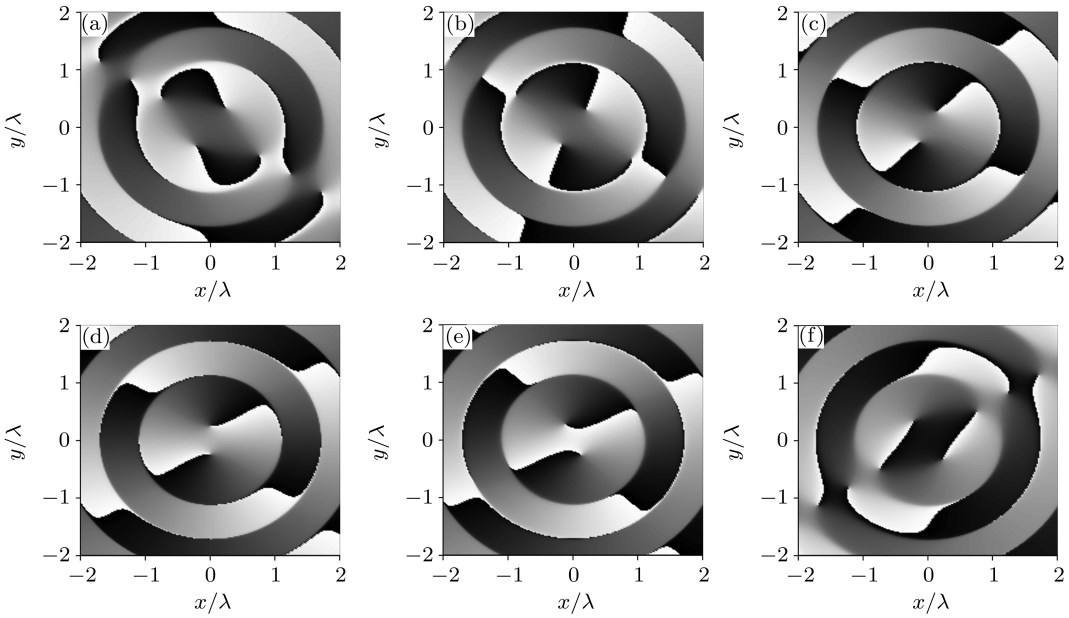


Fig. 5. Influence of varying phase retardation β on phase distributions of $E_z(r, \phi, z)$ with $m = 1$ (RHE-polarised beam) in the focal plane: (a) $\beta = 0$; (b) $\beta = \pi/6$; (c) $\beta = \pi/3$; (d) $\beta = \pi/2$; (e) $\beta = 2\pi/3$; (f) $\beta = \pi$, $E_{0y} = 1.5$. The other parameters are the same as those in Fig. 2.

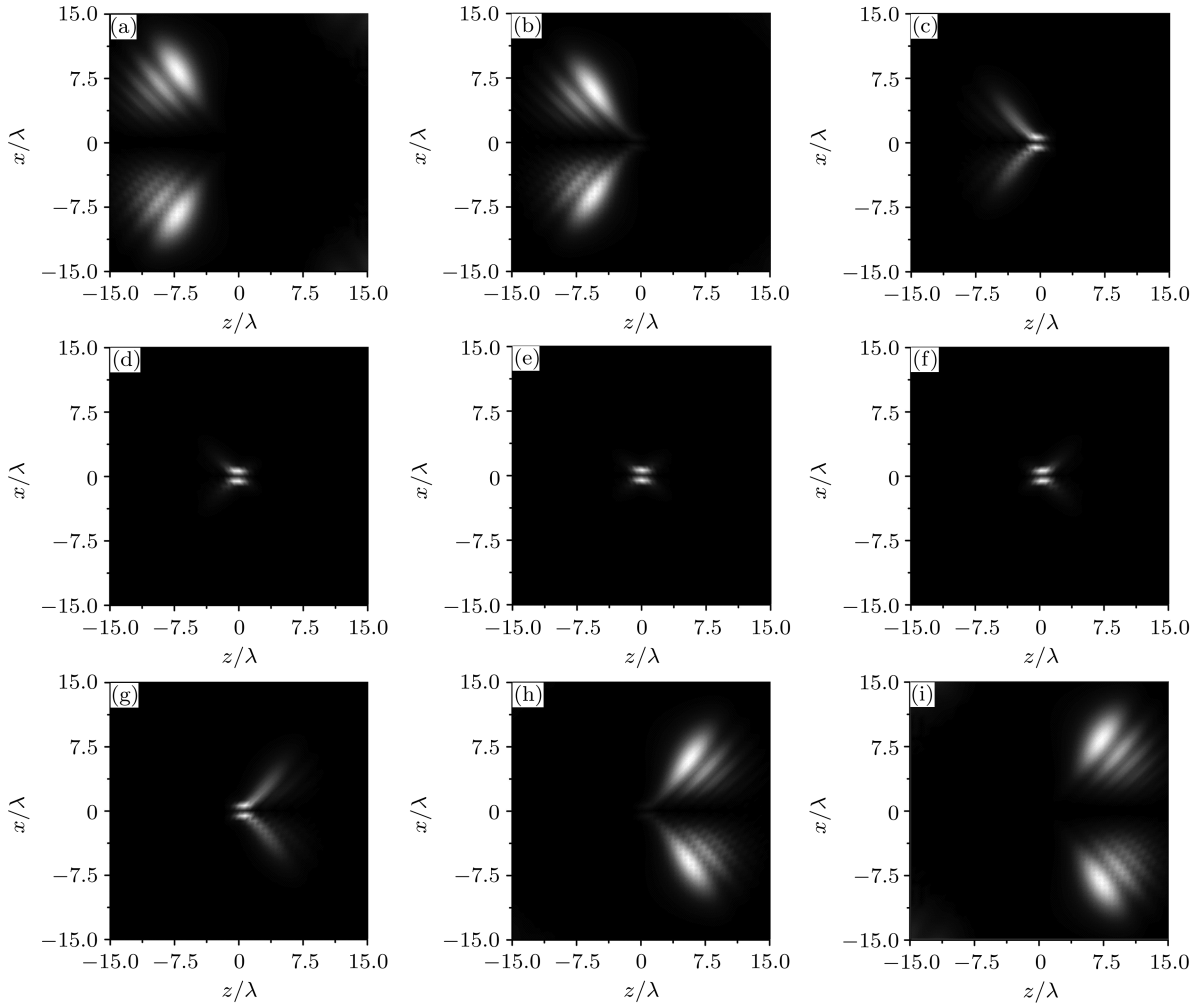


Fig. 6. The propagation evolution of the femtosecond vortex light pulse ($m = 1$ RHE-polarised pulse): (a) $t = -10$ fs; (b) $t = -8$ fs; (c) $t = -5$ fs; (d) $t = -2$ fs; (e) $t = 0$ fs; (f) $t = 2$ fs; (g) $t = 5$ fs; (h) $t = 8$ fs; (i) $t = 10$ fs. The other parameters are chosen to be the same as those in Fig. 2.

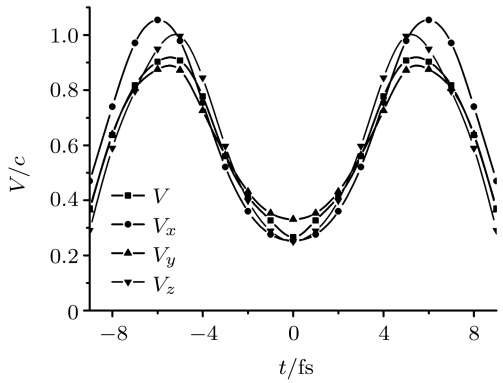


Fig. 7. Pulse group velocity distribution and its x, y and z component velocity distributions near the focus. The parameters are chosen to be the same as those in Fig. 2.

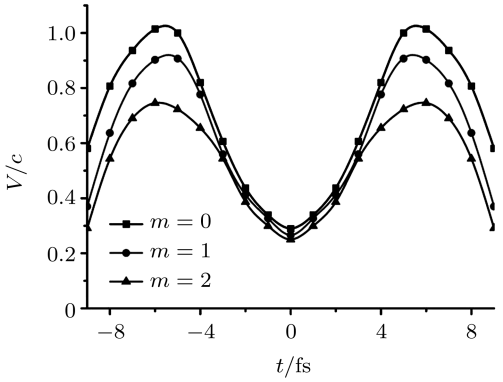


Fig. 8. Pulse group velocity distribution with different topological charges. The other parameters are chosen to be the same as those in Fig. 2.

We present the influence of normalised total AM distribution on the NA of the focusing objective and the pulse duration of the femtosecond vortex light pulse (T) as the vortex light pulse is focused by a high NA objective in Fig. 9. It is seen that the AM increases near the focus and reaches peak on the focal plane. That is because the femtosecond vortex light pulse is focused into a tight spot with intense intensity when the light pulse is focused by a high NA objective and the AM coincides with the intensity distribution. Furthermore, it is obvious that the AM increases with the increment of the NA from Fig. 9(a), and the longer the pulse duration T is, the larger the AM is, as it is shown in Fig. 9(b).

Last but not least, we analysed the normalised total AM distribution at different time in Fig. 10. The value of normalised total AM is lower when the pulse is propagating before or after the focal plane. When the pulse comes to the focal plane, the AM reaches the maximal value. The reason is that the intensity of the light pulse becomes larger when the pulse is closed to the focal plane. Moreover, the further is the pulse away from the focal plane, the smaller the AM is.

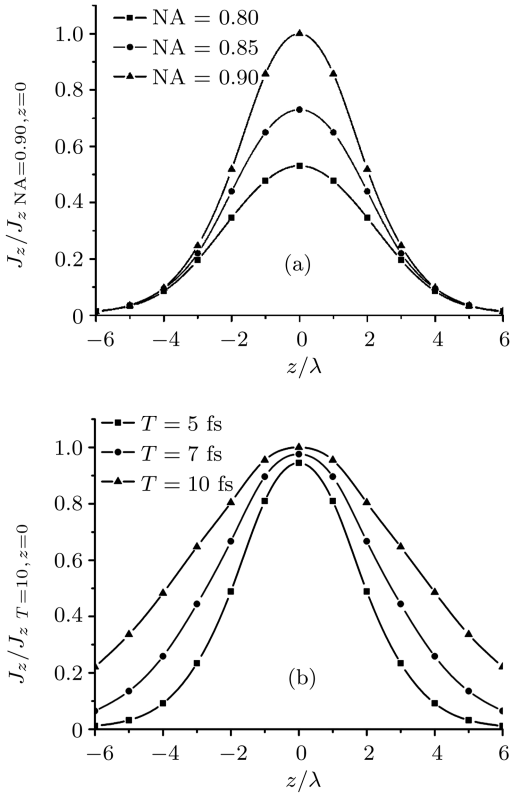


Fig. 9. Influence of AM distribution on (a) NA and (b) T. The other parameters are the same as those in Fig. 2.

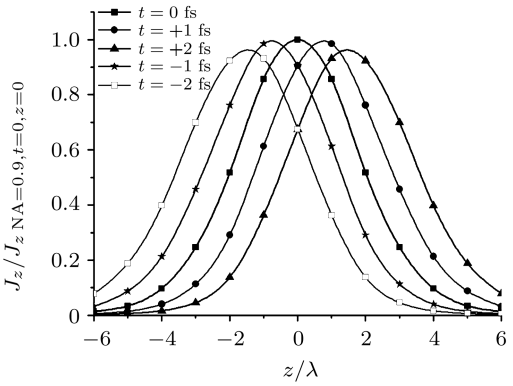


Fig. 10. The AM distribution at different time. The other parameters are the same as those in Fig. 2.

4. Conclusions

We have derived the expressions for the electric field, the group velocity and the total AM of femtosecond elliptically polarised vortex light pulse focused by a high NA objective based on Richards–Wolf vectorial diffraction theory. The intensity distributions in the focal plane with different topological charges are

studied. The phase contours of the z component with different topological charges and phase retardation β, and phase contours of the x, y, and z components with left or right polarised $m = 1$ pulses in the focal plane are illustrated. We found that the propagation group velocity slows down near the focus and becomes faster far away from the focal plane. Moreover, group velocity of elliptically polarised vortex light pulse with the larger topological charge is slower than the smaller ones. Finally, the total AM increases as the NA of the focusing objective increases or as the pulse duration T increases. The results obtained in this paper might be useful in applications of femtosecond elliptically polarised vortex light pulses, such as optical data storage, optical tweezers, etc.

References

[1] Bokor N and Davidson N 2007 *Opt. Commun.* **279** 229
[2] Grosjean T and Courjon D 2007 *Opt. Commun.* **272** 314
[3] Zhang Z, Pu J and Wang X 2008 *Opt. Lett.* **33** 49
[4] Chen B and Pu J 2009 *Appl. Opt.* **48** 1288
[5] Zhang Y L, Zhao Y Q, Zhan Q W and Li Y P 2006 *Acta Phys. Sin.* **55** 1253 (in Chinese)
[6] Youngworth K S and Brown T G 2000 *Opt. Express.* **7** 77
[7] Walker E P and Milster T D 2001 *Proc. SPIE* **4443** 73
[8] Helseth L E 2002 *Opt. Commun.* **212** 343
[9] Lerman G M and Levy U 2007 *Opt. Lett.* **32** 2194
[10] Soskin M S and Vasnetsov M V 2001 *Optics Prog. Opt.* **42** 219
[11] Allen L, Beijersbergen M W, Spreeuw R J C and Woerdman J P 1992 *Phys. Rev.* A **45** 8185
[12] Beijersbergen M W, Allen L, van der Ween H E L O and Woerdman J P 1993 *Opt. Commun.* **96** 123
[13] Cheng K, Liu P S and Lü B D 2008 *Chin. Phys.* B **17** 1743
[14] Foreman M R and Török P 2009 *J. Opt. Soc. Am.* A **26** 2470
[15] Gu M 1999 *Advanced Optical Imaging Theory* (New York: Springer-Verlag, Heidelberg) p166
[16] Richards B and Wolf E 1959 *Proc. Roy. Soc.* A **253** 358
[17] Gori F 1998 *Opt. Lett.* **23** 241
[18] Brixner T, Garcia de Abajo F J, Schneider J and Pferffer W 2005 *Phys. Rev. Lett.* **95** 093901
[19] Bor Z, Gogolak Z and Szabo G 1989 *Opt. Lett.* **14** 862
[20] Brugge D A D and Pukhov A 2009 *Phys. Rev.* E **79** 016603
[21] Romallosa K M, Bantang J and Saloma C 2003 *Phys. Rev.* A **68** 033812
[22] Kempe M, Stamm U and Wilhelmi B 1992 *Opt. Commun.* **89** 119
[23] Helseth L E 2005 *Phys. Rev.* E **72** 047602
[24] Chen X W, Zeng Z N, Dai J, Li X F, Li R X and Xu Z Z 2008 *Chin. Phys.* B **17** 1826
[25] Lu D Q, Hu W, Yang Z J and Zheng Y Z 2004 *Acta Phys. Sin.* **53** 1063 (in Chinese)
[26] Hau L V, Harris S E, Dutton Z and Behroozi C H 1999 *Nature* **397** 594
[27] Bigelow M S, Lepeshkin N N and Boyd R W 2003 *Phys. Rev. Lett.* **90** 113903
[28] Song K Y, Herraez M and Thevenaz G L 2005 *Opt. Express.* **13** 82
[29] Chang-Hasnain C J, Ku P C, Kim J and Chuang S L 2003 *Proc. IEEE* **91** 1884
[30] Zou L F, Bao X Y, Yang S Q, Chen L and Fabien R 2006 *Opt. Lett.* **31** 2698
[31] Bor Z and Horvath Z L 1992 *Opt. Commun.* **94** 249
[32] John W D S 2007 *Appl. Opt.* **46** 7469
[33] Barnett S M and Allen L 1994 *Opt. Commun.* **110** 670